The EMBO Journal vol.15 no.10 pp.2556–2564, 1996

The environment of two metal ions surrounding the splice site of a group I intron

B.Streicher, E.Westhof[1] and R.Schroeder[2]

Institute of Microbiology and Genetics, Vienna Biocenter, Dr Bohrgasse 9, A-1030 Vienna, Austria and [1]Institut de Biologie Moléculaire et Cellulaire du CNRS, F-67084 Strasbourg, France

[2]Corresponding author

Several divalent metal ions (Ca^{2+}, Sr^{2+} and Pb^{2+}) do not promote splicing, but instead induce cleavage at a single site in the conserved group I intron core in the absence of the guanosine cofactor at elevated pH, generating products with 5′-OH and 3′-phosphate ends. The reaction is competed by Mg^{2+}, which does not cleave at this position, but hydrolyses the splice sites producing 3′-OH and 5′-phosphate ends. Mn^{2+} promotes both core cleavage and splice site hydrolysis under identical conditions, suggesting that two different metal atoms are involved, each responsible for one type of cleavage, and with different chemical and geometric requirements. Based on the core cleavage position and on the previously proposed coordination sites for Mg^{2+}, we propose a structural location for two metal ions surrounding the splice site in the Michel–Westhof three-dimensional model of the group I intron core. The proposed location was strengthened by a first mutational analysis which supported the suggested interaction between one of the metal ions and the bulged residue in P7.

Keywords: catalytic RNA/magnesium/manganese/metal ion binding site/RNA structure

Introduction

Catalytic RNAs are metalloenzymes requiring divalent metal ions for two functions: structure stabilization and direct participation in RNA catalysis. Three types of RNA catalysis involving phosphodiester cleavage are known, each requiring divalent metal ions: (i) transesterification as in group I and group II intron splicing; (ii) site-specific hydrolysis as by RNase P and by group I and II introns at the splice sites (ss) resulting in 5′-phosphate and 3′-hydroxyl end groups; and (iii) RNA cleavage as by small ribozymes (e.g. hammerhead, hairpin) leading to 2′3′-cyclic phosphates and 5′-hydroxyls (Cech, 1990; Pan *et al.*, 1993; Pyle, 1993). Metal ions differ in their ability to contribute to catalysis. For the group I intron-derived *Tetrahymena* ribozyme, it was shown that Mg^{2+} and Mn^{2+} promote the endonuclease cleavage analogous to the first step of splicing, whereas Ca^{2+}, Sr^{2+} and Ba^{2+} can only contribute to folding (Grosshans and Cech, 1989).

The mapping of RNA-bound metal ions proves difficult. Crystallographic studies identified metal binding sites in tRNAs (Holbrook *et al.*, 1977; Hingerty *et al.*, 1978; Quigley *et al.*, 1978; Westhof and Sundaralingam, 1986) and the hammerhead ribozyme (Pley *et al.*, 1994; Scott *et al.*, 1995). For large RNAs, however, functional assays are used to detect essential metal ion–RNA contacts. In group I introns, a phosphorothioate interference study identified pro-Rp phosphate oxygens which contact essential Mg^{2+} ions in the *Tetrahymena* intron (Christian and Yarus, 1992, 1993; Waring, 1989). However, this technique cannot distinguish between ions essential for folding or for catalysis. In another approach, incorporation of a sulfur atom instead of the 3′-bridging oxygen at the cleavage site of the *Tetrahymena* ribozyme rendered the substrate resistant to cleavage in the presence of Mg^{2+}; however, cleavage could be partially rescued by the addition of Mn^{2+}. This metal specificity switch suggests a direct metal ion coordination to this bridging oxygen (Piccirilli *et al.*, 1993).

We previously showed that Pb^{2+} cleaves specifically the core of group I introns (Streicher *et al.*, 1993). In yeast $tRNA^{Phe}$, crystallographic studies revealed that the binding site for a Pb^{2+} ion, which specifically cleaves the tRNA, overlaps with a strong Mg^{2+} binding site (Brown *et al.*, 1983, 1985; Rubin and Sundaralingam, 1983). We therefore concluded that a specific Pb^{2+} cleavage site in a structured RNA might not only be indicative of a distinct Pb^{2+} binding site nearby, but also of a high affinity Mg^{2+} binding site. However, Pb^{2+} is not able to fold the group I intron RNA into a splicing-competent conformation. Here we used site-specific cleavage of group I intron RNA by divalent ions, which are able to fold the intron RNA, to localize high affinity metal ion binding sites. Based on experimental data, a first three-dimensional model including two metal ions which surround the splice site is proposed. The strength of this approach lies in the possibility of stepwise refinement by an alternation of experiments and structural modelling.

Results

Cleavage of the td intron core by Ca^{2+}, Sr^{2+} and Mn^{2+}

Ca^{2+} and Sr^{2+} cannot promote the guanosine-dependent splicing reaction of group I introns (Grosshans and Cech, 1989). However, in the absence of the guanosine cofactor at pH values higher than for splicing, preRNA of the *td* intron is cleaved specifically by Ca^{2+} or Sr^{2+}, giving rise to two prominent products differing from those of splicing (Figure 1A, lanes 4–6). Under similar conditions, site-specific hydrolysis by Mg^{2+} occurs predominantly at the splice sites, resulting in products similar to those of splicing (Inoue *et al.*, 1986; Figure 1A, lane 2). Mn^{2+} has an intermediate status, since it promotes both 5′ss hydrolysis as does Mg^{2+}, and cleavage as do Ca^{2+} and Sr^{2+} (Figure 1A, lane 3). The concentration of divalent metal ions required for site-specific cleavage is in the

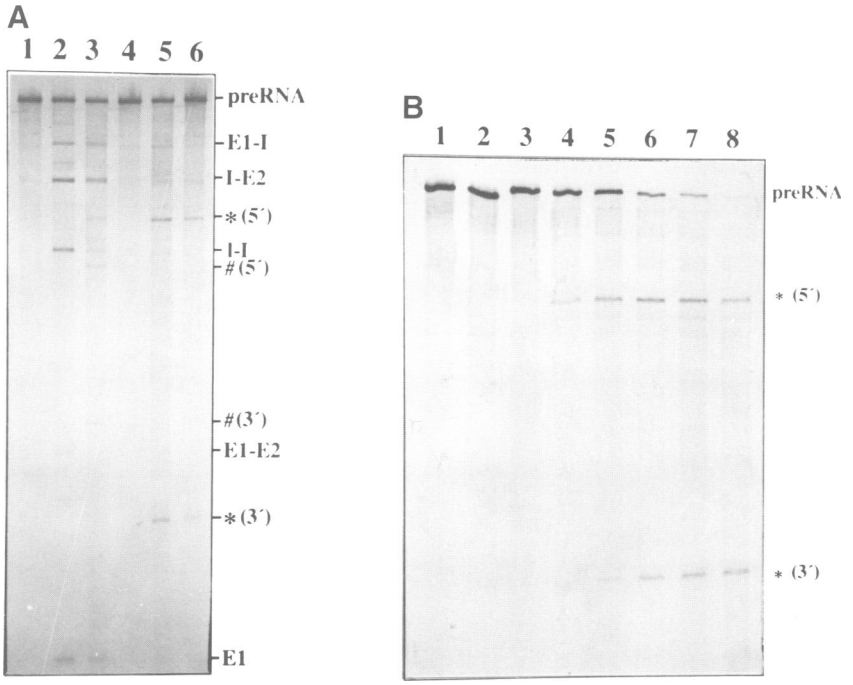

Fig. 1. Characterization of site-specific cleavage reactions in the absence of the guanosine cofactor. (**A**) Cleavage of *td* precursor RNA (preRNA) by different divalent metal ions. Cleavage of ^{35}S-labelled preRNA was performed with 5 mM metal chloride at 37°C for 30 min at pH 8.0 (lanes 1–3) or 90 min at pH 9.0 (lanes 4–6). Lanes 1 and 4, no metal added; lane 2, $MgCl_2$; lane 3, $MnCl_2$; lane 5, $CaCl_2$; and lane 6, $SrCl_2$. Bands are labelled E1-I (5′ exon–intron), I-E2 (intron–3′ exon), I-I (linear intron), E1-E2 (ligated exons), E1 (5′ exon) for products of splice site hydrolysis and * for core cleavage. # indicate additional cleavage products infrequently obtained with $MnCl_2$ (5′ of A906). (**B**) Time course. A typical cleavage experiment with 5 mM $CaCl_2$ at pH 9.0 incubated for 1.5, 5, 10, 30, 70 min or 3, 7, 9 h (lanes 1–8). Bands are labelled as in (A).

same range as the concentration of Mg^{2+} necessary for the splicing reaction. Kinetic experiments revealed k_{obs} values of 2.8×10^{-3}/min or 2×10^{-4}/min for the Ca^{2+}- or Sr^{2+}-dependent cleavages at 5 mM metal chloride, respectively. This cleavage rate is 1500- or 100-fold higher than that of non-specific hydrolysis, which was calculated as 1.9×10^{-6}/min for an average position (see Figure 1B).

Mapping the cleavage site

The position for Ca^{2+}-, Sr^{2+}- and Mn^{2+}-induced cleavages, mapped by primer extension (Figure 2A), is 5′ to U940 in J8/7 in the conserved intron core. As shown in the secondary structure (Figure 2B), this corresponds to the position where Pb^{2+} cleaves the wild-type intron in the presence of Mg^{2+} (Streicher *et al.*, 1993). Since a metal-induced site-specific cleavage indicates a metal binding site in the vicinity, the cleavages observed suggest the existence of a metal binding pocket around this position which can accommodate various divalent ions. Indeed, while Mg^{2+} does not cleave at position U940 even after long incubation times (data not shown), cleavage by Ca^{2+} and Sr^{2+} can be competed by the addition of Mg^{2+} (Figure 3). A ribozyme version of the *td* intron lacking the first seven nucleotides was also cleaved specifically by Ca^{2+} and Sr^{2+} at U940 (data not shown), indicating that neither the exons nor the paired P1 stem are essential for formation of this metal binding site. Moreover, addition of the splicing cofactor GTP up to a concentration of 1 M did not influence core cleavage by Ca^{2+} and Sr^{2+} (data not shown).

Terminal groups of cleavage products

Cleavage of RNA by divalent metal ions such as in small ribozymes proceeds via activation of an internal nucleophile, the 2′-OH of the ribose adjacent to the cleavage site, leading to a 2′3′-cyclic phosphate and a 5′-hydroxyl end. Site-specific hydrolysis by Mg^{2+} at the splice sites in group I and group II introns as well as cleavage of a pre-tRNA by RNase P uses water as the nucleophile and results in 3′-hydroxyl and 5′-phosphate groups (Cech, 1993; Pan *et al.*, 1993; Pyle, 1993). To classify the type of cleavage we observed, we determined the ends of the cleavage products by radioactive labelling of free hydroxyl ends. The results are summarized in Figure 4. Cleavage by Mg^{2+} and Mn^{2+} at the splice sites results in 3′-hydroxyls and 5′-phosphates, as expected from the ability of the products to perform further reactions requiring a 3′-OH (second step of splicing, circularization; Inoue *et al.*, 1986). However, cleavage within the core by Ca^{2+}, Sr^{2+} and Mn^{2+} resulted in 5′-hydroxyl ends and a phosphate at the 3′ end. Thus, the two types of site-specific cleavage can occur in group I introns. Note that Mn^{2+} is able simultaneously to perform either type of cleavage (5′ss hydrolysis and core cleavage). The pH values optimal for site-specific hydrolysis by different metal ions reflect their p*K*a values, suggesting that, as proposed for Pb^{2+} cleavage in tRNA (Brown *et al.*, 1983) and the

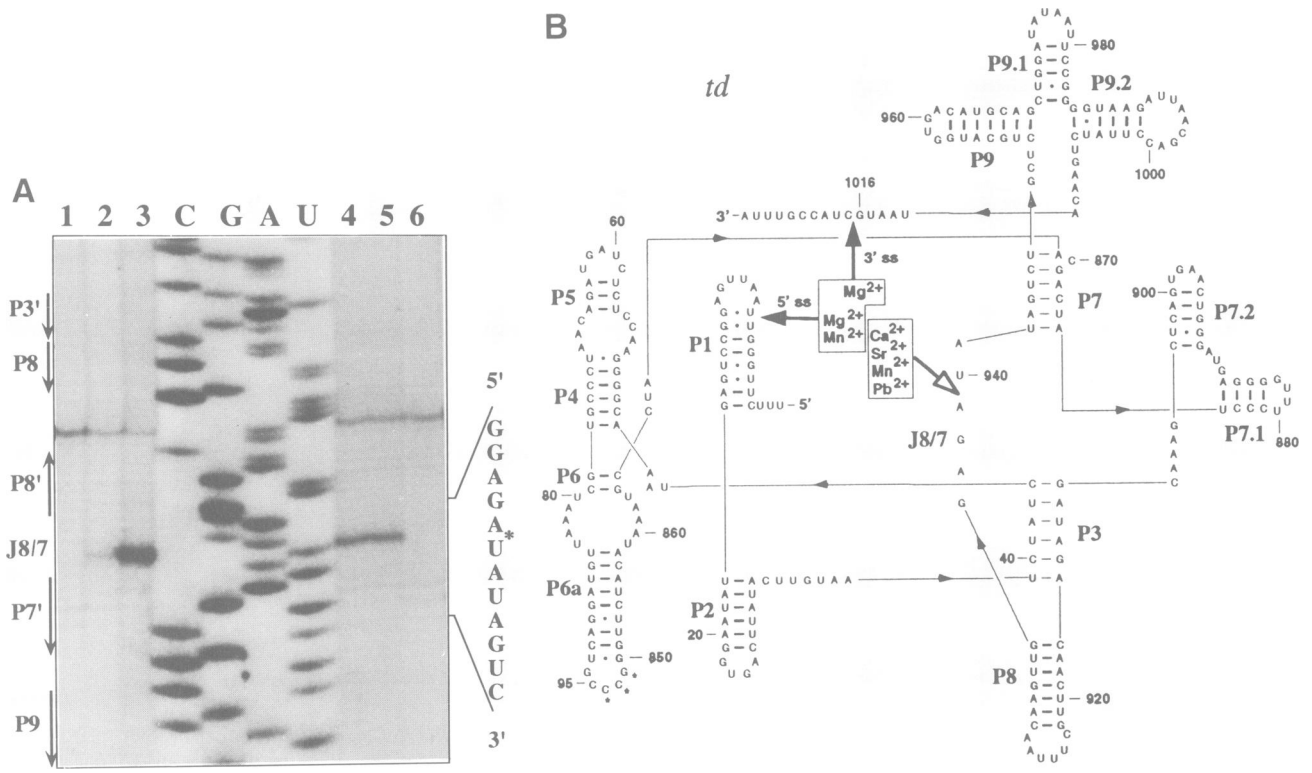

Fig. 2. (**A**) Localization of cleavage sites. Primer extension of preRNA cleaved with 0, 3 or 5 mM $CaCl_2$ (lanes 1–3) or 10, 5 or 0 mM $SrCl_2$ (lanes 4–6) at pH 9.0 for 60 min. CGAU denotes sequencing lanes. The sequence around the cleavage site 5′ to U940 in J8/7 (*) and the positions of the stems are indicated. (**B**) Secondary structure of the T4 phage-derived *td* intron (adapted from Cech *et al.*, 1994 with XRNA). Cleavage sites are indicated by filled arrows for hydrolysis at the splice sites and an open arrow for core cleavage 5′ to U940. P1–P9.2 designate the stems; 5′ss and 3′ss are the splice sites. Bases marked with * denote the position of the open reading frame deleted in the construct used (Schroeder *et al.*, 1991).

hammerhead ribozyme reaction (Dahm *et al.*, 1993), the active species is a metal hydroxide ion.

Folding of the intron RNA is similar with Mg^{2+} and Ca^{2+}

To assess whether the two types of site-specific cleavage observed reflect different foldings depending on the specific ionic conditions used for these cleavages, we performed structural probing. RNA was renatured in the presence of either Mg^{2+} or Ca^{2+}, subjected to dimethylsulfate (DMS) modification and the sites accessible to modification were determined by primer extension. The protections seen in Figure 5 (in comparison with EDTA-denatured RNA) show that secondary as well as tertiary structure elements are well formed in the presence of either ion and that no significant differences between the structures formed in Mg^{2+} or Ca^{2+} could be detected. This demonstrates that the presence of Ca^{2+} does not induce a different conformation leading to core cleavage, but rather different binding, without significantly altering the structure. Ca^{2+} thus supports the splicing-competent structure of the intron. In accordance, at suboptimal Mg^{2+} concentrations, low amounts of Ca^{2+} enhance the first step of splicing in the *td* intron (data not shown) and in the *Tetrahymena* intron (Grosshans and Cech, 1989). Increasing amounts of Ca^{2+}, however, inhibit splicing, preferentially the second step (data not shown).

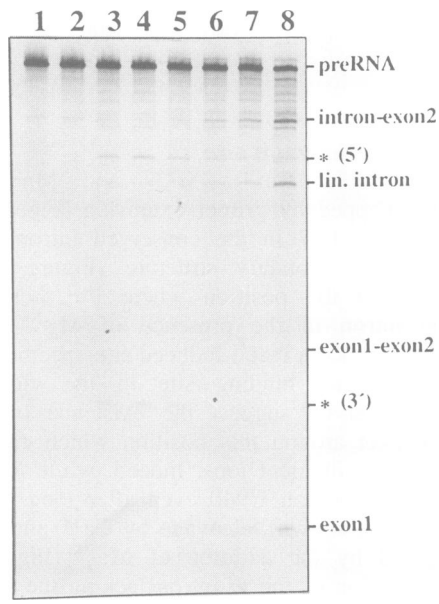

Fig. 3. Competition of $CaCl_2$ and $MgCl_2$ cleavage in the absence of guanosine. Reactions were performed at pH 8.5 as described in Figure 1A in the presence of 0, 1, 3 or 5 mM $CaCl_2$ (lanes 1–4). Lanes 5–8 included 5 mM $CaCl_2$ and, additionally, 1, 3, 5 or 10 mM $MgCl_2$. Products of core cleavage are labelled with *.

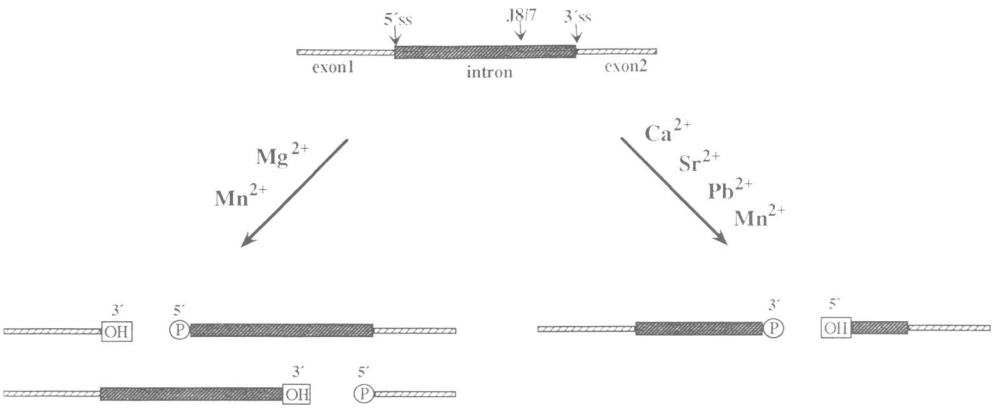

Fig. 4. Cleavage at different sites by divalent metal ions generates products with opposite end groups. A circled P indicates a (5′, 3′ or 2′3′-cyclic) phosphate end; a boxed OH a terminal hydroxyl group. 5′ss and 3′ss are the splice sites.

Positioning metal ions in the 3D model

The facts that (i) no difference can be observed in the folding induced by Mg^{2+} and Ca^{2+} and (ii) that Mn^{2+} promotes two types of cleavage at different sites under identical conditions suggest that two separate metal ion binding sites are involved. To assess this hypothesis, the current three-dimensional (M–W) model (Michel and Westhof, 1990) was used to visualize hydrated metal ions in positions allowing them to perform core cleavage and splice site hydrolysis. The position of core cleavage by Ca^{2+}, Sr^{2+}, Mn^{2+} or Pb^{2+} (5′ to U940) is surprisingly close to the splice site in the M–W model. However, the two cleavage sites are too far apart to rationalize cleavage by a single metal ion, but require the assumption of two metal ion binding pockets, each potentially harbouring a metal ion responsible for one type of cleavage. The proposed binding pockets (Figure 6A and B) are in the catalytic core, close to the splice site and on opposite sides of the guanosine cofactor bound to the G binding site (Michel *et al.*, 1989). Phosphorothioate substitution experiments in the *Tetrahymena* intron suggested that several phosphates need to bind Mg^{2+} as a prerequisite for splicing (Waring, 1989; Christian and Yarus, 1992, 1993). Three of the phosphates exhibiting the highest sensitivity towards thioate substitution, phosphates U940, A941 and A943 in *td* nomenclature, were used to coordinate the two modelled metal ions.

Metal ion A

One of the positioned ions, referred to as A, was modelled contacting the 3′-hydroxyl of the guanosine cofactor (if present) and the phosphate 5′ to A941 in J8/7, the equivalent of which was suggested to interact with a Mg^{2+} ion by phosphorothioate interference experiments in the *Tetrahymena* intron (Christian and Yarus, 1993). A further contact involves the N3 position of C870, the bulged nucleotide 5′ to the G binding site in P7. Thus, metal ion A has position, distance and geometry suitable to cleave the splice site.

Metal ion B

The second metal ion, designated B, was modelled contacting the phosphates 5′ to U940 and A943 in J8/7, both of which were suggested previously to coordinate Mg^{2+} via their pro-Rp oxygens (Christian and Yarus, 1993).

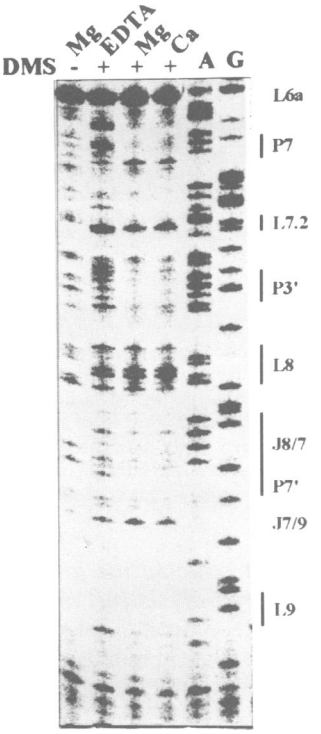

Fig. 5. Primer extension of RNA modified with DMS under different ionic conditions. The ribozyme construct of the *td* intron tdL-7 was renatured in the presence of 20 mM $MgCl_2$ or $CaCl_2$ or denatured in the presence of 20 mM EDTA. Modification was performed at room temperature at pH 7.4, i.e. conditions where Ca^{2+} cleavage is not observed. The gel shows part of the intron, with regions marked on the right. Protection of positions induced by folding with Mg^{2+} or Ca^{2+} in comparison with the denatured state can be seen in stems (e.g. P3, P7) and loops involved in tertiary interactions (L9). A and G are sequencing lanes.

Coordination to the phosphate 5′ to U940 makes site B a reasonable candidate for cleavage at this position when it is occupied by Ca^{2+}, Sr^{2+}, Mn^{2+} or Pb^{2+}. A cleavage site does not automatically indicate coordination to that position. However, in this special case, J8/7 forms a sharp turn in this region, thus by itself creating a potential metal ion binding pocket (Michel and Westhof, 1990; Figure 6A and B). Additionally, ion B is close to the 3′-bridging oxygen of the splice site, which was proposed to contact a Mg^{2+} ion directly (Piccirilli *et al.*, 1993).

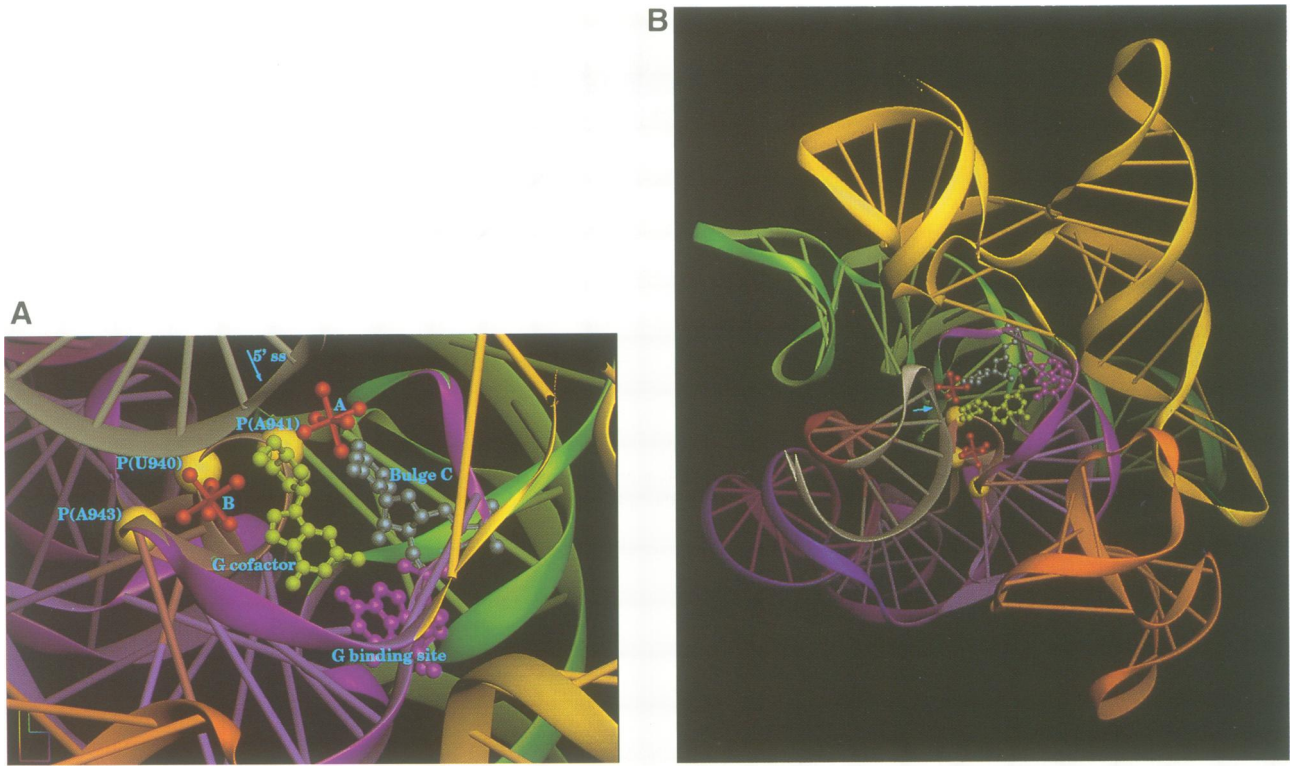

Fig. 6. (**A**) Local view of the proposed metal ion binding pockets in the 3D model of the catalytic core of bacteriophage T4 *td* intron prior to the first step of splicing. The base pairs are represented by solid bars and the sugar-phosphate backbone by a ribbon. The P1 helix is in grey and the 5′ splice site is indicated by a blue arrow. The phosphates equivalent to those presenting a phosphorothioate effect in the *Tetrahymena* ribozyme (Christian and Yarus, 1992) are denoted and represented by yellow spheres. The hydrated A and B magnesium ions (in red, at the centre of an octahedron with one water molecule at each apex 2 Å away) are positioned on each side of the ribose of the guanosine cofactor which is depicted at the centre of the view in yellow–green colour (it is in hydrogen bonding position to the G of the G binding site shown in purple as the whole P7 helix). The bulge C residue is shown in silver and the J8/7 segment in orange. In green is shown part of the P6 helix and in yellow part of the P9.0 helix. Some contacts between the magnesium ions and the RNA are possibly made directly after removal of one or more water molecules. At the present stage, it would be unrealistic to attempt to identify those direct contacts and to give precise distances between the partners around the catalytic site. (**B**) Global view of the catalytic site within the whole *td* intron. Same colour code as in (A). The P9 extension is at the top right in yellow and the P7 extension is at the bottom right in red–orange. Behind at the top left, in green, can be seen the P5 helix. The modelling is based on the model of the *sunY* intron (Jaeger *et al.*, 1993). All drawings were made with DRAWNA (Massire *et al.*, 1994).

Mutating the bulged nucleotide in P7 (C870) affects splice site hydrolysis but not core cleavage

To test the proposed coordination of metal ion A to the bulged nucleotide 5′ to the G binding site (C870), mutants at this position were compared for their cleavage activities with Mg^{2+} and Ca^{2+} (Figure 7 and Table I). Mutation of this base in the *td* intron results in increased Mg^{2+} requirements for splicing and an elevated K_m for GTP (Schroeder *et al.*, 1991). All four constructs were cleaved well at position U940 with Ca^{2+} (k_{obs} values differing at most 2-fold), but mutants C870U and C870G were up to 10-fold down in Mg^{2+} hydrolysis at the splice sites (Schroeder *et al.*, 1991). Thus, only splice site hydrolysis by Mg^{2+} is severely affected by this mutation, consistent with the notion that ion A is responsible for splice site hydrolysis by Mg^{2+}, but not for core cleavage by Ca^{2+}. In the presence of Mg^{2+}, Pb^{2+} weakly cleaves the phosphodiester bond 5′ to the bulged nucleotide in the mutated form C→U (Streicher *et al.*, 1993), suggesting that the mutation leads to a locally distorted metal ion A site. In accordance with the proposed coordination of ion A to the ring nitrogen of the bulged nucleotide, those constructs where the ring nitrogen of the base is accessible, C (N3) and A (N1), are more active in splice site hydrolysis. In addition, the bulged nucleotide is semi-conserved as C or A in all group I introns (Michel and Westhof, 1990).

Discussion

Different metal ions exhibit different activities in the group I intron RNA. Table II summarizes the abilities of the tested divalent metal ions to perform folding, splicing and site-specific cleavage. All divalent metal ions tested except Pb^{2+} fold the intron RNA in a splicing-competent fashion (Grosshans and Cech, 1989). Only Mg^{2+} efficiently promotes both steps of splicing.

A general metal ion binding pocket

Metal ions have the ability to cleave the RNA backbone when bound to a strong binding site with a suitable geometry for attacking the 2′-OH ribose group or the phosphate group (Behlen *et al.*, 1990). We used this property to trace high affinity metal ion binding sites in the T4 phage-derived *td* intron. A single prominent metal ion cleavage event was found in the core (5′ to U940), which is promoted by Ca^{2+}, Sr^{2+}, Mn^{2+} (Figure 1A, lanes 5, 6 and 3) and, as previously observed, by Pb^{2+} (Streicher *et al.*, 1993). This indicates that a general metal ion binding pocket exists in the vicinity of that cleavage site. Mg^{2+} does not cleave this position, but competes with Ca^{2+}, thus inhibiting core cleavage (Figure 3). Phosphorothioate substitution experiments suggested Mg^{2+} coordination to the cleaved phosphate (Christian and

Yarus, 1993). Thus, we propose that Mg^{2+} binds to this same general binding site, but with a geometry different from that of the other ions and not suitable for core cleavage. This is reminiscent of the overlapping binding sites for Pb^{2+} and Mg^{2+} in yeast $tRNA^{Phe}$, where the two ions cleave at different positions in the D-loop (Brown *et al.*, 1983, 1985; Rubin and Sundaralingam, 1983; Ciesiolka *et al.*, 1989).

The similar structural probing data for intron RNA folded in the presence of Mg^{2+} or Ca^{2+} show that it is unlikely that the different cleavages observed result from altered folding induced by the different metal ions. In addition, both types of cleavage can occur in the presence of either only Mn^{2+} or both Ca^{2+} and Mg^{2+} simultaneously (Figure 3). Moreover, Pb^{2+} cleaves at the same position as Ca^{2+}, Sr^{2+} and Mn^{2+} in the intron core, but requires Mg^{2+} for folding (Streicher *et al.*, 1993). Recent work on non-self-splicing mitochondrial group I introns of *Neurospora crassa* demonstrated that these introns require the CYT-18 protein for tertiary structure formation, as determined by various structural probing methods. In that instance, Pb^{2+} cleavage in J8/7 was only detected in the presence of CYT-18 protein, verifying that this reaction indeed requires the correct splicing-competent tertiary structure (Caprara *et al.*, 1996). These results strengthen our interpretation that the different cleavages we observe with different metal ions result from distinct binding properties of the ions to defined metal ion binding pockets.

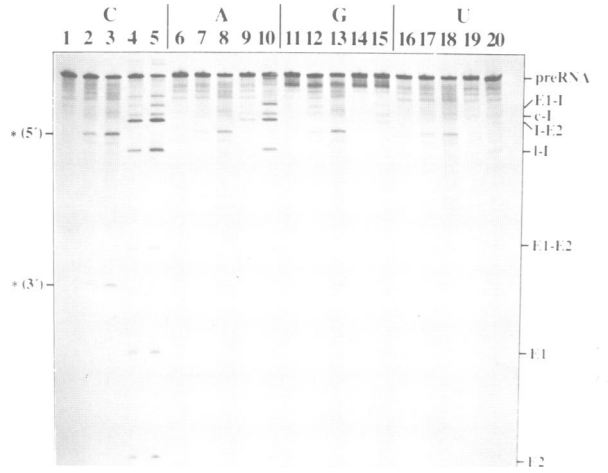

Fig. 7. Effects of mutation of C870 on Ca^{2+} and Mg^{2+} cleavage in the absence of the guanosine cofactor. Lanes 1–5 show wild-type C870, lanes 6–10 mutant C870A, lanes 11–15 mutant C870G and lanes 16–20 mutant C870U. PreRNA was cleaved with 0, 1 or 5 mM $CaCl_2$ (lanes 1–3, 6–8, 11–13 and 16–18) or 3 and 5 mM $MgCl_2$ (lanes 4–5, 9–10, 14–15 and 19–20) at pH 9.0 for 30 min. Bands are labelled as in Figure 1A with c-I (circular intron), E2 (3′ exon).

Table I. k_{obs} values ($\times 10^{-3}$/min) for Mg^{2+}-induced splice site hydrolysis and Ca^{2+}-induced core cleavage as determined for the mutants at C_{870}

	C (wt)	A	U	G
Ca^{2+}	2.8	2.0	2.2	1.5
Mg^{2+}	25.3	30	5.9	2.6

A model for two metal ions, A and B, close to the splice site

To accommodate metal ions responsible for Ca^{2+}-, Sr^{2+}- or Mn^{2+}-promoted core cleavage and Mg^{2+}- or Mn^{2+}-induced splice site hydrolysis in the 3D model (Michel and Westhof, 1990), we propose that two metal ion binding pockets are involved, harbouring the metal ions for the different reactions. From the positions of the cleavages and of the phosphate groups most sensitive to thioate substitution (Waring, 1989; Christian and Yarus, 1992, 1993), the two ions appear in close proximity to each other and close to the splice site in the M–W model (Figure 6A and B). According to this positioning, one of the two ions, referred to as A, is responsible for Mg^{2+}-dependent hydrolysis at the splice sites and is coordinated to the phosphate 5′ to A941 and the ring nitrogen of the bulged nucleotide (C870) 5′ to the G binding site. The second ion, designated B, is responsible for core cleavage by Ca^{2+}, Sr^{2+}, Mn^{2+} and Pb^{2+}, and is coordinated to the phosphates 5′ to U940 and A943 and to the 3′-bridging oxygen of the splice site. The latter has been proposed to coordinate directly a Mg^{2+} ion (Piccirilli *et al.*, 1993). The two metal ions coordinate all three phosphates shown to coordinate Mg^{2+} ions by phosphorothioate substitution experiments in the *Tetrahymena* intron as a prerequisite for splicing (Waring, 1989; Christian and Yarus, 1992, 1993). Further support for the suggested coordinations was provided by a mutational study: mutation of a proposed ligand for ion A (N3 of C870) affected only splice site hydrolysis, the type of cleavage attributed to ion A, but not core hydrolysis attributed to ion B (Figure 7).

Involvement of two metal ions in splicing?

The positioning of two ions in the 3D model resembles the two metal ion mechanism established for the 3′-5′-exonuclease activity of Klenow polymerase (Freemont *et al.*, 1988; Beese and Steitz, 1991) and proposed by Steitz and Steitz (1993) as a general model for reactions of catalytic RNAs (Figure 8A). However, the distance

Table II. Functions performed by different divalent ions on the *td* intron

Metal ion	Folding	Splicing		Site-specific cleavage		
		1st step	2nd step	5′ Splice site 5′-P/3′-OH	3′ Splice site 5′-P/3′-OH	J8/7 5′-OH/3′-P
Mg^{2+}	+	+	+	+	+	–
Mn^{2+}	+	+	–	+	±	+
Ca^{2+}	+	–	–	–	–	+
Sr^{2+}	+	–	–	–	–	+
Pb^{2+}	–	–	–	–	–	+[a]

[a]In mutant C870U, an additional cleavage is observed 5′ to U870 (Streicher *et al.*, 1993).

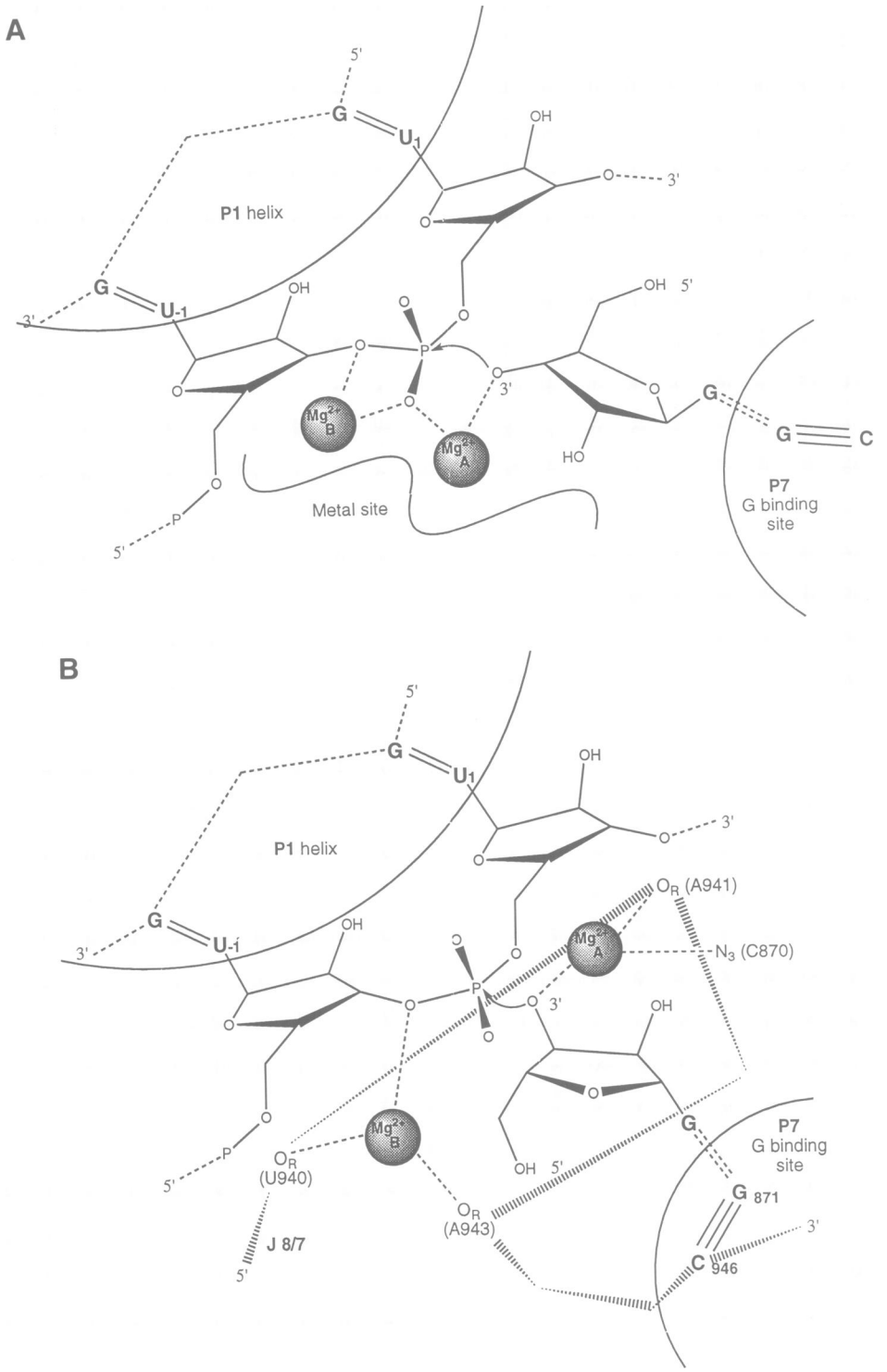

Fig. 8. (**A**) Schematic view illustrating the positions of the two metal ions in the catalytic site of group I introns according to the Steitz and Steitz (1993) hypothesis. Notice that the O4′ of the ribose of the guanosine substrate points away from the viewer and the O3′ points to the viewer. (**B**) Schematic view illustrating the positions of the two metal ions in the catalytic site of group I introns according to the present proposal (compare Figure 6A). The serpentine path of the J8/7 segment is delineated by striped bars, whose width indicates the proximity to the viewer. Notice that now the O4′ atom of the ribose of the G cofactor is pointing towards the viewer. Proposed coordinations of the metal ions to phosphates and base C870 discussed in the text are indicated. The nomenclature is that of the *td* intron.

between the two positioned ions in our model is 8.6 Å and, although at this stage of modelling and refinement this distance is subject to variation, it is more than twice the distance obtained from the suggested analogy (Steitz and Steitz, 1993). One possible origin for the distance difference might lie in the relative positions of the reacting nucleotides. In the polymerases, the bases linked to the reacting phosphodiesters stack on each other, the nucleo-

tides are in helical continuity and the diphosphates protrude off the helix (Steitz *et al.*, 1994). In the group I introns, it is a nucleotide, external to the helix, whose ribose attacks a phosphodiester within the helical substrate (Cech, 1993). The position of the G cofactor in the first step of splicing is similar to that of the last G residue of the intron in the second step of splicing as given by the M–W model (Michel and Westhof, 1990). In the M–W model, the position of the last G residue is dictated by the G binding site in P7, the stacking of P9.0 on P7 and the fact that P9.0 and P10 are in the same region of space with respect to the G binding site. With such a topological arrangement of the chains, the G cofactor sugar could not be oriented as shown in Figure 8A. In addition, a rotation of the base with respect to the glycosyl bond need not be envisaged, since it has been shown that the guanosine substrate is bound in the *anti* conformation (Lin *et al.*, 1994). Finally, compared with the polymerase situation, the sugar of the guanosine substrate is in the location of a Mg^{2+} ion (site A in Figure 8A), while site A of the intron is not far from the position of the diphosphate of the dNTP of the polymerase reaction (Figure 8B).

Following the Steitz and Steitz model, for the first step of splicing, ion A would activate the nucleophile, the 3′-hydroxyl of the guanosine cofactor, to attack the splice site, whereas ion B would stabilize the negative charge developing on the leaving group. For the second step of splicing, the two ions would exchange their roles (Steitz and Steitz, 1993). Detailed kinetic measurements on the *Tetrahymena* ribozyme lead to the suggestion that two Ca^{2+} ions compete with two Mg^{2+} ions for the chemical step (McConnell, 1995). Thus, it is tempting to consider whether the two ions we inferred from metal-induced cleavages could be responsible for the proposed functions during splicing. The first step of splicing is promoted by Mg^{2+} and Mn^{2+}. The second step, however, is only promoted by Mg^{2+} in the *td* intron (data not shown). A property shared by Mg^{2+} and Mn^{2+} is the induction of splice site hydrolysis, which we attributed to ion A. In contrast, of these two ions, only Mn^{2+} induces core cleavage, assigned to ion B. Ca^{2+} enhances splicing at suboptimal Mg^{2+} concentrations, but inhibits at higher concentrations, preferentially the second step. Our experiments do not allow conclusions on the roles of ions A and B in splicing; however, one could hypothesize that core cleavage by Mn^{2+}, Ca^{2+}, Sr^{2+} or Pb^{2+} reflects binding of these ions to site B but with a coordination not suitable for the second step of splicing.

Materials and methods

RNA preparation

Precursor RNA (preRNA) of the T4 phage-derived thymidylate synthase (*td*) intron was *in vitro* transcribed with [α-^{35}S]CTP and purified as described (Streicher *et al.*, 1993) from plasmid *td* ΔP6-2 T (Schroeder *et al.*, 1991), containing 100 nucleotides (nt) as the 5′-exon, 265 nt intron and 56 nt as the 3′-exon. Ribozyme construct tdL-7 lacks the first seven bases of the intron (Heuer *et al.*, 1991) and was prepared by transcription under hydrolysis conditions (pH 8.0, 15 mM $MgCl_2$).

Site-specific hydrolysis

Approximately 20 nmol of ^{35}S-labelled preRNA were renatured in buffer containing 50 mM Tris–HCl (pH 8.0 for Mg^{2+} and Mn^{2+}; pH 9.0 for Ca^{2+} and Sr^{2+}), 0.4 mM spermidine and usually 5 mM metal chloride at 56°C for 2 min and subsequently incubated at 37°C for the time indicated in the figures. The reaction was stopped by addition of formamide-containing gel loading buffer or ethanol precipitation and products were separated on 5% denaturing polyacrylamide gels.

Primer extension

Metal ion-cleaved preRNA was ethanol precipitated and used as the template for primer extension performed in buffer containing 100 mM Tris–HCl pH 8.4, 10 mM $MgCl_2$, 0.25 mM dNTP with AMV reverse transcriptase for 60 min at 42°C with ^{32}P-end-labelled oligo *td*-3′I (5′-CATTATGTTCAGATAAGGTCG-3′). Reaction products were ethanol precipitated and separated on 6 or 8% polyacrylamide gels.

Determination of cleavage product ends

The end groups for the individual reaction products were determined by their ability to be labelled by [γ-^{32}P]ATP (→free 5′-OH) or by [α-^{32}P]pCp (→free 3′-OH). ^{35}S-Body-labelled preRNA was cleaved by different divalent metal ions and subjected to (i) 5′-end-labelling with [γ-^{32}P]ATP and T4 polynucleotide kinase in buffer containing 0.1 M Tris–HCl pH 8.0, 5 mM dithiothreitol, 10 mM $MgCl_2$, 0.2 mM spermidine for 60 min at 37°C and (ii) 3′-end-labelling with [α-^{32}P]pCp and T4 RNA ligase in buffer containing 50 mM Tris–HCl pH 7.8, 10 mM $MgCl_2$, 1 mM β-mercaptoethanol, 1 mM ATP for 2 h at 37°C. Products were ethanol precipitated and analysed on a 5% polyacrylamide gel in parallel with unlabelled reactions.

DMS modification

The freshly transcribed tdL-7 ribozyme was folded by addition of buffer (50 mM Tris-Cl pH 7.4, 0.4 mM spermidine, 0.1 mM EDTA, 0.1 mM EGTA) and divalent metal ions (20 mM) and incubation at 56°C for 2 min followed by slow cooling to room temperature. EDTA-containing reactions were heated to 90°C for 2 min followed by immediate cooling on ice. DMS modification was performed in 50 µl reactions with 1 µl of a 20-fold dilution of DMS in ethanol for 10 min at room temperature, stopped by addition of β-mercaptoethanol and precipitated. Modified RNAs were used as templates for primer extension reactions.

Kinetics

The k_{obs} values were calculated as the slopes of plotting time versus activity expressed as the percentage of 5′ or 3′ product of total counts. For the determination of the unspecific cleavage rate, the amount of precursor plus product bands was expressed as a percentage of total radioactivity of a given lane. The slope of this linear decrease (k_{obs} of 5×10^{-4}/min) was divided by the number of positions where hydrolysis could occur. Values were obtained by scanning polyacrylamide gels of time course hydrolysis reactions using a Molecular Dynamics PhosphorImager and were corrected for non-specific hydrolysis.

Acknowledgements

We thank V.Lehnert for preparing Figure 6, C.Massire for help with the DRAWNA program (Massire *et al.*, 1994), B.Weiser for the XRNA program, and U.von Ahsen, M.G.Wallis, H.Wank and A.Barta for stimulating discussions. This work was supported by Austrian Science Foundation Grant PO9853-MOB to R.S. and European Community Grant Bio2-CT93-0345 to E.W and R.S.

References

Beese,L.S. and Steitz,T.A. (1991) *EMBO J.*, **10**, 25–33.
Behlen,L.S., Sampson,J.R., DiRenzo,A.B. and Uhlenbeck,O.C. (1990) *Biochemistry*, **29**, 2515–2523.
Brown,R.S., Hingerty,B.E., Dewan,J.C. and Klug,A. (1983) *Nature*, **303**, 543–546.
Brown,R.S., Dewan,J.C. and Klug,A. (1985) *Biochemistry*, **24**, 4785–4801.
Caprara,M., Mohr,G. and Lambowitz,A.M. (1996) *J. Mol. Biol.*, **257**, 512–531.
Cech,T.R. (1990) *Annu. Rev. Biochem.*, **59**, 543–568.
Cech,T.R. (1993) In Gesteland,R.F. and Atkins,J.F. (eds), *Structure and Mechanism of Large Catalytic RNAs: Group I and Group II Introns and Ribonuclease P.* Cold Spring Harbor Laboratory Press, Plainview, NY, pp. 239–269.
Cech,T.R., Damberger,S.H. and Gutell,R. (1994) *Nature Struct. Biol.*, **1**, 273–280.
Christian,E.L. and Yarus,M. (1992) *J. Mol. Biol.*, **228**, 743–758.
Christian,E.L. and Yarus,M. (1993) *Biochemistry*, **32**, 4475–4480.

Ciesiolka,J., Wrzesinski,J., Gornicki,P., Podkowinski,J. and Krzyzosiak,W.J. (1989) *Eur. J. Biochem.*, **186**, 71–77.
Dahm,S.A.C., Derrick,W.B. and Uhlenbeck,O.C. (1993) *Biochemistry*, **32**, 13040–13045.
Freemont,P.S., Friedman,J.M., Beese,L.S., Sanderson,M.R. and Steitz,T.A. (1988) *Proc. Natl Acad. Sci. USA*, **85**, 8924–8928.
Grosshans,C.A. and Cech,T.R. (1989) *Biochemistry*, **28**, 6888–6894.
Heuer,T.S., Chandry,P.S., Belfort,M., Celander,D.W. and Cech,T.R. (1991) *Proc. Natl Acad. Sci. USA*, **88**, 11105–11109.
Hingerty,B., Brown,R.S. and Jack,A. (1978) *J. Mol. Biol.*, **124**, 523–534.
Holbrook,S.R., Sussman,J.L., Warrant,R.W., Church,G.M. and Kim,S.-H. (1977) *Nucleic Acids Res.*, **4**, 2811–2820.
Inoue,T., Sullivan,F.X. and Cech,T.R. (1986) *J. Mol. Biol.*, **189**, 143–165.
Jaeger,L., Westhof,E. and Michel,F. (1993) *J. Mol. Biol.*, **234**, 331–346.
Lin,C.W., Hanna,M. and Szostak,J.W. (1994) *Biochemistry*, **33**, 2703–2707.
Massire,C., Gaspin,C. and Westhof,E. (1994) *J. Mol. Graph.*, **12**, 201–206.
McConnell,T.S. (1995) *Involvement of Guanosine and Mg^{2+} in the Tetrahymena Ribozyme Reaction*. University of Colorado.
Michel,F. and Westhof,E. (1990) *J. Mol. Biol.*, **216**, 585–610.
Michel,F., Hanna,M., Green,R., Bartel,D.P. and Szostak,J.W. (1989) *Nature*, **342**, 391–395.
Pan,T., Long,D.M. and Uhlenbeck,O.C. (1993) In Gesteland,R.F. and Atkins,J.F. (eds), *Divalent Metal Ions in RNA Folding and Catalysis*. Cold Spring Harbor Laboratory Press, Plainview, NY, pp. 271–302.
Piccirilli,J.A., Vyle,J.S., Caruthers,M.H. and Cech,T.R. (1993) *Nature*, **361**, 85–88.
Pley,H.W., Flaherty,K.M. and McKay,D.B. (1994) *Nature*, **372**, 68–74.
Pyle,A.M. (1993) *Science*, **261**, 709–714.
Quigley,G.J., Teeter,M.M. and Rich,A. (1978) *Proc. Natl Acad. Sci. USA*, **75**, 64–68.
Rubin,J.R. and Sundaralingam,M. (1983) *J. Biomol. Struct. Dyn.*, **1**, 639–646.
Schroeder,R., von Ahsen,U. and Belfort,M. (1991) *Biochemistry*, **30**, 3295–3303.
Scott,W.G., Finch,J.T. and Klug,A. (1995) *Cell*, **81**, 991–1002.
Steitz,T.A. and Steitz,J.A. (1993) *Proc. Natl Acad. Sci. USA*, **90**, 6498–6502.
Steitz,T.A., Smerdon,S.J., Jäger,J. and Joyce,C.M. (1994) *Science*, **266**, 2022–2025.
Streicher,B., von Ahsen,U. and Schroeder,R. (1993) *Nucleic Acids Res.*, **21**, 311–317.
Waring,R.B. (1989) *Nucleic Acids Res.*, **17**, 10281–10293.
Westhof,E. and Sundaralingam,M. (1986) *Biochemistry*, **25**, 4868–4878.

Received on July 3, 1995; revised on January 3, 1996